TOXICOLOGICAL SCIENCES 115(1), 253–266 (2010)
doi:10.1093/toxsci/kfq021
Advance Access publication January 27, 2010

Development of a Quantitative Model Incorporating Key Events in a Hepatotoxic Mode of Action to Predict Tumor Incidence

Nicholas S. Luke,* Reeder Sams II,† Michael J. DeVito,‡ Rory B. Conolly,§ and Hisham A. El-Masri§,[1]

*Department of Mathematics, North Carolina Agricultural and Technical State University, Greensboro, North Carolina 27411; †National Center for Environmental Assessment, Office of Research and Development, U.S. Environmental Protection Agency, Research Triangle Park, North Carolina 27711; ‡National Toxicology Program, National Institute for Environmental Health Sciences, Research Triangle Park, North Carolina 27709; and §Integrated Systems Toxicology Division, National Health and Environmental Effects Research Laboratory, Office of Research and Development, U.S. Environmental Protection Agency, Research Triangle Park, North Carolina 27711

[1] To whom correspondence should be addressed at U.S. Environmental Protection Agency, 109 T.W. Alexander Drive, Mail Drop B143-01, Research Triangle Park, NC 27711. Fax: (919) 541-4284. E-mail: el-masri.hisham@epa.gov.

Received September 4, 2009; accepted January 20, 2010

Biologically based dose-response (BBDR) modeling of environmental pollutants can be utilized to inform the mode of action (MOA) by which compounds elicit adverse health effects. Chemicals that produce tumors are typically labeled as either genotoxic or nongenotoxic. Though both the genotoxic and the nongenotoxic MOA may be operative as a function of dose, it is important to note that the label informs but does not define a MOA. One commonly proposed MOA for nongenotoxic carcinogens is characterized by the key events cytotoxicity and regenerative proliferation. The increased division rate associated with such proliferation can cause an increase in the probability of mutations, which may result in tumor formation. We included these steps in a generalized computational pharmacodynamic (PD) model incorporating cytotoxicity as a MOA for three carcinogens (chloroform, $CHCl_3$; carbon tetrachloride, CCL_4; and N,N-dimethylformamide, DMF). For each compound, the BBDR model is composed of a chemical-specific physiologically based pharmacokinetic model linked to a PD model of cytotoxicity and cellular proliferation. The rate of proliferation is then linked to a clonal growth model to predict tumor incidences. Comparisons of the BBDR simulations and parameterizations across chemicals suggested that significant variation among the models for the three chemicals arises in a few parameters expected to be chemical specific (such as metabolism and cellular injury rate constants). Optimization of model parameters to tumor data for CCL_4 and DMF resulted in similar estimates for all parameters related to cytotoxicity and tumor incidences. However, optimization of the $CHCl_3$ data resulted in a higher estimate for one parameter (*BD*) related to death of initiated cells. This implies that additional steps beyond cytotoxicity leading to induced cellular proliferation can be quantitatively different among chemicals that share cytotoxicity as a hypothesized carcinogenic MOA.

Key Words: quantitative modeling; risk assessment; mode of action.

General scientific consensus is that the current risk assessment methodologies and approaches are insufficient with respect to efficiently characterizing the human health risk of exposure to existing and future environmental pollutants (Collins *et al.*, 2008). Current approaches must move toward risk assessment methodologies that will assess the risk to multiple environmental pollutants or classes of chemicals simultaneously (Edwards and Preston, 2008). The National Research Council (NRC, 2007) has made multiple recommendations regarding the approach to human health risk assessment. Among these recommendations and key to characterizing, the dose-response paradigm is the use of computational modeling or biologically based dose-response (BBDR) models. BBDR models may be designed and developed as computational tools to test mode of action (MOA) hypotheses and characterize uncertainty (e.g., extrapolation, human variation, duration of exposure, etc.) across classes of environmental pollutants.

In recent years, MOA analysis has become a useful tool in human health risk assessment to inform the approach for low-dose extrapolation of risk (Meek *et al.*, 2003; Slikker *et al.*, 2004a; Sonich-Mullin *et al.*, 2001; U.S. Environmental Protection Agency [USEPA], 2005) and a critical component of BBDR models. Throughout the evolution of risk assessment methodologies, many MOAs have been proposed and commonalities in the general mode(s) of action are being realized. Among these commonalities is the cytotoxic MOA leading to tumor formation (Slikker *et al.*, 2004b). Specifically, for this MOA, the key events for either the parent chemicals or their bioactive metabolites are identified as (1) exposure to an environmental pollutant, (2) sustained cellular cytotoxicity, (3) regenerative cell proliferation, and (4) tumor formation.

The Environmental Protection Agency's Cancer Guidelines (USEPA, 2005) emphasize the use of MOA information in risk assessment for environmental pollutants to better characterize the risk of adverse health effects to humans. In addition, when available, the use of a BBDR model is generally preferred because empirical data are used to characterize the

pharmacokinetic and pharmacodynamic (PD) relationships of the key events in MOA rather than default assumptions. Significant progress has been made in utilizing pharmacokinetic models in risk assessments (Thompson *et al.*, 2008). In comparison, the use of PD models is not as prevalent because they are heavily dependent upon MOA information, which is often inadequate for environmental pollutants. Therefore, a key question arises, "how can BBDR modeling efforts inform missing information (e.g. MOA)?" In part, iterative modeling processes can be utilized to test MOA hypotheses, identify research gaps, and generate data to parameterize the BBDR model. Model predictions could provide agreement with empirical data, providing support for the hypothesized MOA. Conversely, if model fits are inconsistent with data across chemicals, then the model can be used to identify research needs for specific chemicals and classes of chemicals. It is important to note that modeling efforts of this type (i.e., BBDR) can only test MOA hypotheses and not identify alternative MOA(s). Future steps must consider the use of relevant phenotypic measurements representing key events, the source and magnitude of model uncertainty, uncertainty derived from the MOA, and variation in physiological or biochemical parameters.

Multiple environmental pollutants including chloroform ($CHCl_3$) (Wolf and Butterworth, 1997), carbon tetrachloride (CCl_4) (Manibusan *et al.*, 2007), furan (Moser *et al.*, 2009), dimethylarsinic acid (Cohen *et al.*, 2007), and N,N-dimethylformamide (DMF) (Ohbayashi *et al.*, 2008), among many others, are believed to induce a tumorigenic response through a cytotoxic MOA. Tumors that are hypothesized to be induced through a cytotoxic MOA have been observed in multiple tissues, including liver (Holsapple *et al.*, 2006), bladder (Cohen *et al.*, 2007), and kidney (Hard, 2002). Several of the compounds mentioned here are hypothesized to induce tumors through this MOA, induce their toxic effect in the liver as a target organ. Development of a computational model for key events within the MOA is dependent upon the availability of sufficient empirical data. Hepatocellular cytotoxicity is typically measured by several laboratory methods, including histopathological techniques and serum liver enzymes. Likewise, cellular regeneration within the liver can also be evaluated by histopathological techniques in addition to bromodeoxyuridine (BrdU) and radioactive labeling techniques to measure the synthesis of DNA in proliferating liver cells. Empirical data to support key events must demonstrate both a dose-response and a temporal relationship for the formation of hepatocellular tumors (USEPA, 2005). For many environmental pollutants, sufficient empirical data to evaluate a hepatocellular cytotoxic MOA is unavailable; however, considerable data for $CHCl_3$ (USEPA, 2001), CCL_4 (USEPA, 2008), and DMF (Senoh *et al.*, 2004) exist to support the development of a BBDR model for a cytotoxic MOA.

For these three compounds, it is logical to hypothesize that a quantifiable relationship may exist between each of the key events as well as with the tumor response. Holsapple *et al.* (2006) stated, "it is important to establish that there are parallel dose responses (not necessarily identical) for the key events (i.e., cytotoxicity and proliferation) and tumors, as well as specificity of the key events and the tumor response." Additionally, it is critical to evaluate whether other MOAs contribute significantly to the tumorigenic response, although this was not possible within this BBDR effort. The testing of alternative MOA(s) would require empirical data to test such hypotheses. Previously, a physiologically based pharmacokinetic/PD (PBPK/PD) model was developed for $CHCL_3$, which is hypothesized to act through a cytotoxic MOA (Tan *et al.*, 2003). For these reasons, we have expanded upon this work by developing a BBDR model to predict the tumorigenic response based upon the key events of cytotoxicity and cellular proliferation for $CHCl_3$, CCl_4, and DMF. The purpose of the modeling effort in this paper was to develop a generalized computational model incorporating key events in a cytotoxic MOA for tumorgenicity. A comparison of the optimized PD parameters for cytotoxicity and tumor incidence will indicate the ability to generalize this MOA across these chemicals. This model describes the relationship between cytotoxicity, regenerative proliferation, and tumorigenic response. If the proposed hypothesis of cytotoxicity leading to regenerative proliferation and tumor formation is correct for all chemicals examined, then the only chemical-specific model parameters needed should be those that relate chemical exposure (pharmacokinetics) to cytotoxicity. Once chemical-specific processes cause cytotoxicity, numerical magnitude of resulting regenerative proliferation and tumors should be independent of chemical in a generalized cytotoxicity MOA for tumorgenicity.

MATERIALS AND METHODS

Software

The model was coded and simulations were executed using MATLAB R2006b (The Mathworks Inc., Natick, MA). The systems of differential equations were integrated using the MATLAB command *ode15s*, which uses a variable order method to solve a system of stiff differential equations. All simulations were run on a 2.8 GHz Pentium computer running the Windows XP operating system.

Data reported in previously published studies were digitized *via* the DataThief III v1.1 (Bas Tummers, Eindhoven, the Netherlands) digitization program.

Model Structure

The overall BBDR model has been formulated to link exposure to a compound with the probability of forming hepatocellular tumors in female B6C3F1 mice. For the three chemicals, $CHCl_3$, CCl_4, and DMF, hepatic metabolic activity is related to the formation of tumors (Manibusan *et al.*, 2007; Ohbayashi *et al.*, 2008; Wolf and Butterworth, 1997). Therefore, PBPK models were utilized from literature for CCl_4 and $CHCl_3$ and developed *de novo* for DMF to estimate the rate of metabolism in the liver. The metabolism rate was then used as an input to a PD model of cytotoxicity and regenerative proliferation to estimate a proliferation rate for use in a two-stage clonal growth model to predict the formation of tumors. The following sections provide a detailed description of the structure of the overall model structure (depicted in Fig. 1).

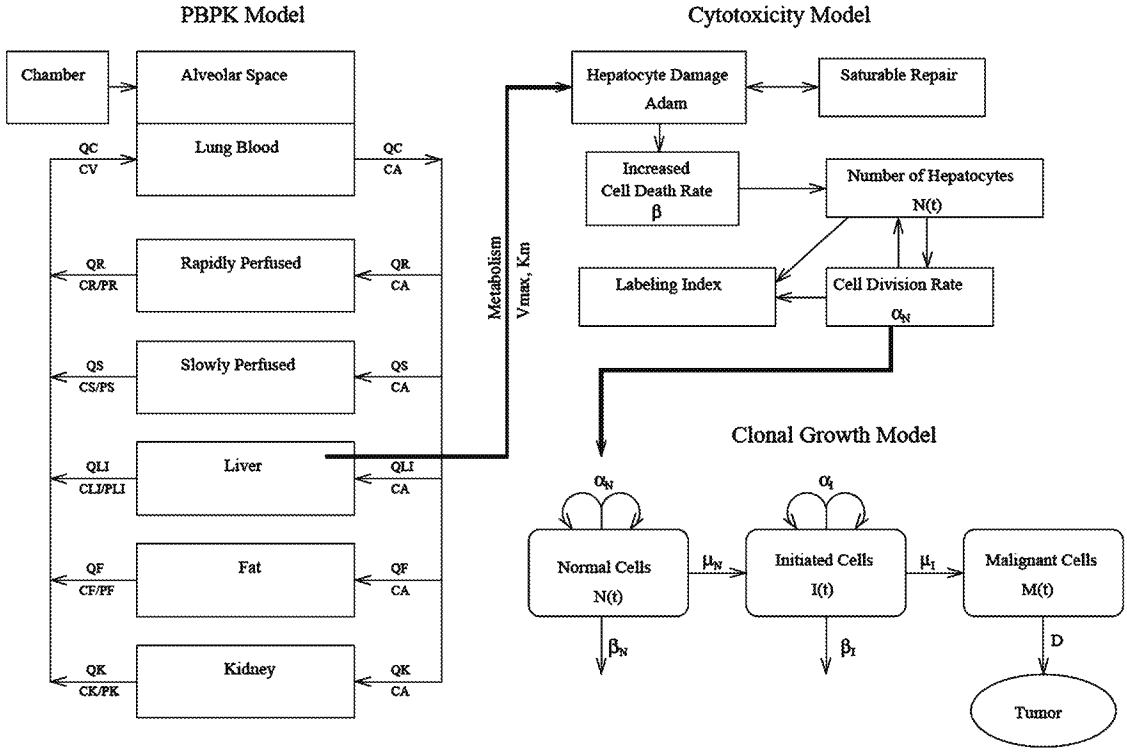

FIG. 1. Schematic drawing of the overall BBDR model. A PBPK model is linked to a PD model of cytotoxicity and regenerative proliferation that is also linked with a two-stage clonal growth model.

PBPK models. For each compound, a PBPK model was used to approximate the metabolism rate in the liver. Each model was constructed with the same general structure, which was similar to the model developed for styrene by Ramsey and Andersen (1984). The general structure of the PBPK model is represented by Equations A1–A9 in the Appendix. All three models included compartments for lung, liver, fat, slowly perfused tissues, and rapidly perfused tissues. The models for $CHCl_3$ and DMF also included an additional compartment for the kidney. A kidney compartment was included in the DMF model to incorporate available urinary excretion data for model development.

It is assumed that all three compounds are metabolized in the liver and that $CHCl_3$ is also metabolized in the kidney (Branchflower *et al.*, 1984). Hepatic metabolism was described as a single metabolic pathway that followed Michaelis-Menten kinetics. In addition to hepatic metabolism, DMF urinary excretion was included in the DMF PBPK model as a first order process.

The PBPK model parameter values for each compound are displayed in Table 1. The $CHCl_3$ model was reproduced using values reported in Corley *et al.* (1990) and Tan *et al.* (2003). Parameter values for CCl_4 were taken from Benson *et al.* (2001) and Thrall *et al.* (2000). A PBPK model for DMF was not located, thus the PBPK model parameters were obtained from literature or optimized as described.

Physiological parameter (volumes and blood flows) values from the $CHCl_3$ model were also used for the DMF model and were supplemented with values reported in Brown *et al.* (1997) when necessary. DMF partition coefficients were estimated from the DMF octanol:water coefficient, log $K_{OW} = -1.01$ (Gluck *et al.*, 1996), using an algorithm developed by Poulin and Krishnan (1995). For DMF hepatic metabolism, the Michaelis constant (K_m) was recalculated (unit conversion) from Mraz *et al.* (1993), while the maximum rate (V_{max}) was optimized to DMF plasma concentration levels from a 6-h inhalation exposure study presented by Hundley *et al.* (1993).

PD model of cytotoxicity. The PD model of cytotoxicity and regenerative proliferation was based on the models of cytotoxicity and regenerative proliferation presented in Tan *et al.* (2003) and Liao *et al.* (2007). Conceptually, the cytotoxicity model related the rate of damage formation in the liver proportionally to the PBPK model–predicted rate of hepatic metabolism. Damage was removed (repaired) by a saturable repair process. As the damage accumulate and surpassed a threshold, the cellular death rate increased. To compensate for an increase in cell death, regenerative proliferation occurred, leading to an increased division rate. Equations A10–A15 in the Appendix represent these processes.

Regenerative proliferation is a compensatory action in a cytotoxicity MOA. That is, the cellular division rate increases to compensate for an increased cellular death rate. Cellular death rate was linked to chemical dose *via* the rate of chemical metabolism and hepatocyte damage. Thus, as the chemical dose and metabolism increased, the amount of hepatocyte damage increased, leading to an increase in both the cellular death and the division rates. We included a maximal death rate (β_{max}, defined to be 50% of the maximal division rate) in the PD cytotoxicity model because sufficiently high chemical doses resulted in death rates much greater than the maximal division rate, causing a depletion of the cell population. In the MOA examined here, depletion of the cell population was not biologically plausible. Additionally, because the labeling index (represented by Equation A15) is computed by dividing the number of labeled cells by the total number of cells, a depletion of the cell population would lead to an undefined labeling index, resulting in a mathematical error. For these reasons, we elected to incorporate a maximal death rate, as detailed above. It should be noted that the assumption that the maximal death rate is 50% of the maximal division rate was arbitrarily chosen based on analysis of several values between 25 and 150% of the maximal division rate. Values within this examined range exhibited no impact on the overall model predictions.

Parameter values used in the cytotoxicity model for each compound are displayed in Table 2. Values used in the $CHCl_3$ model were taken from Tan *et al.* (2003) and Liao *et al.* (2007) and verified by comparing the model output to labeling index data reported in Larson *et al.* (1996). Parameters that represent cellular processes (e.g., saturable repair, division, and death rates) were assumed to have the same value in the models for all three chemicals. The

TABLE 1
Parameter Values for the PBPK Models (optimized and estimated values are italicized)

Parameter	Function	$CHCl_3$	CCl_4	DMF
BW	Body weight of mouse (kg)	0.0255[a]	0.025[b]	0.0255[a]
V_{LI}	Volume of liver (% BW)	5.86[c]	4[b]	5.86[c]
V_K	Volume of kidneys (% BW)	1.7[c]	n/a	1.7[c]
V_F	Volume of fat (% BW)	6.0[c]	4[b]	6.0[c]
V_{LU}	Volume of lungs (% BW)	n/a	n/a	0.73[d]
V_R	Volume—rapidly perfused tissue (% BW)	3.3[c]	5[b]	2.27[e]
V_S	Volume—slowly perfused tissue (% BW)	74.14[c]	78[b]	74.14[c]
Q_L	Alveolar ventilation (l/h)	2.01[c]	1.8[b]	2.01[c]
Q_C	Cardiac output (l/h)	2.01[c]	1.8[b]	2.01[c]
Q_{LI}	Blood flow to liver (%Q_C)	25[c]	24[b]	25[c]
Q_K	Blood flow to kidney (%Q_C)	25[c]	n/a	25[c]
Q_F	Blood flow to fat (%Q_C)	2[c]	5[b]	2[c]
Q_R	Blood flow to rapidly perfused (%Q_C)	29[c]	52[b,i]	29[c]
Q_S	Blood flow to slowly perfused (%Q_C)	19[c]	19[b]	19[c]
P_{LI}	Liver:blood partition coefficient (unitless)	0.7012[a]	3.142[b]	*0.94*[f]
P_K	Kidney:blood partition coefficient (unitless)	0.5062[a]	n/a	*0.96*[f]
P_F	Fat:blood partition coefficient (unitless)	10.04[c]	62.17[b]	*0.28*[f]
P_R	Rapidly perfused:blood partition (unitless)	0.7925[c]	3.142[b]	*0.94*[f]
P_S	Slowly perfused:blood partition (unitless)	0.5394[c]	1.004[b]	*0.82*[f]
V_{max}	Maximal rate of metabolism (mg/h)	0.6421[a]	0.0605[b]	*1.085*[g]
K_m	Half-maximal concentration (mg/l)	0.77[a]	0.46[b]	14.2[h]
A	Constant relating metabolic activity of kidney to metabolic activity of liver (unitless)	0.153[c]	n/a	n/a
k_{loss}	Chemical loss due to chamber leak (%)	n/a	5[b]	n/a
k_U	Urinary excretion rate constant (l/h)	n/a	n/a	8.5×10^{-5}[g]

Note. n/a, not applicable.
[a]Tan *et al.* (2003).
[b]Benson and Springer (1999).
[c]Corley *et al.* (1990).
[d]Brown *et al.* (1997).
[e]Corley *et al.* (1990), adjusted for lung volume.
[f]Estimated using algorithm presented by Poulin and Krishnan (1995).
[g]Optimized to data (Hundley *et al.*, 1993).
[h]Mraz *et al.* (1993).
[i]Blood flow to the kidneys is incorporated into the rapidly perfused tissue, as there was no kidney compartment in the CCl_4 PBPK model.

proportionality constant (k_{dam}) relating the rate of metabolism to the amount of cellular damage is a chemical-specific parameter.

The value of k_{dam} for $CHCl_3$ was obtained from Tan *et al.* (2003). For CCl_4, k_{dam} was optimized by fitting the model results to labeling index data presented in Benson and Springer (1999) (http://www.osti.gov/em52/final_reports/54940.pdf). Without labeling index data, k_{dam} for DMF was optimized, in conjunction with the clonal growth model, to tumor incidence data (Seno*h et al.*, 2004).

Clonal growth model. Tumor incidences for each chemical were predicted using a two-stage clonal growth model. The biological structure of this model was similar to other two-stage models (also known as MVK models) that have recently been presented (Andersen and Conolly, 1998; Crump *et al.*, 2005; Kodell *et al.*, 2001; Little *et al.*, 2008). Our model considered three independent populations of cells (normal, initiated, and malignant cells). The population dynamics of normal and initiated cells were governed by the following events:

- A normal cell can replicate with probability α_N resulting in two normal cells.
- A normal cell can differentiate or die with probability β_N.
- A normal cell can mutate with probability μ_N yielding one normal cell and one initiated cell.
- An initiated cell can replicate with probability α_I resulting in two initiated cells.
- An initiated cell can differentiate or die with probability β_I.
- An initiated cell can mutate with probability μ_I yielding one initiated cell and one malignant cell.

The parameters for the division (α_N) and death (β_N) of normal cells were calculated by the cytotoxicity model. The mutation probability (μ_N) was set so that the model predicted a basal or background level of tumor incidence in absence of chemicals. As doses of each chemical were introduced in the model, simulations were first run under the assumption that both the division and the death rates of initiated cells were the same as for normal cells, and the resulting predicted tumor incidences did not exhibit much of an increase above basal. This suggested that the initiated cells required a growth advantage over normal cells to result in an increased tumor incidence in the presence of chemicals. Computationally, this growth advantage can be incorporated as an increase in the division rate or as a decrease in the death rate of initiated cells.

Recent studies suggest that the levels of cytochrome P450 2E1 (CYP2E1), the primary enzyme responsible for the metabolism of $CHCl_3$, CCl_4, and DMF, are reduced in initiated and cancerous cells (Bergheim *et al.*, 2007; Ho *et al.*, 2004). We assumed that the reduced level of CYP2E1 would decrease the rate of metabolism in initiated cells, thereby lessening the cytotoxicity and ensuing death rate. This was incorporated into the model by setting the death rate of initiated cells equal to the death rate of normal cells in the absence of chemical. In the presence of chemical, the death rate is then multiplied by a reduction factor (BD, where $0 \leq BD \leq 1$). This reduction in death rate effectively gives the population of initiated cells a growth advantage, similar to that described by Conolly *et al.* (2003).

Hence, the division (α_I) and death (β_I) rate parameters for initiated cells are given by the following equations:

$$\alpha_I(t) = \alpha_N(t) \tag{1}$$

$$\beta_I(t) = \begin{cases} \beta_N(t) & \text{if dose } = 0 \\ \beta_N(t) \cdot BD & \text{if dose } > 0 \end{cases}. \tag{2}$$

Furthermore, the mutation parameters for initiated and normal cells are assumed to be the same.

Because several of the parameters used in this model are time dependent, we utilize a version of the clonal growth model based on earlier published formulation (Portier *et al.*, 1996, 2000). The structure of this model is as follows:

$$\frac{dP_N(s,T)}{ds} = \alpha_N(T-s)P_N^2(s,T) + \beta_N(T-s) + \mu_N(T-s)P_N(s,T)P_I(s,T) - [\alpha_N(T-s) + \beta_N(T-s) + \mu_N(T-s)]P_N(s,T) \tag{3}$$

TABLE 2
Parameter Values for the PD Model of Cytotoxicity and Regenerative Proliferation (optimized values are in bold)

Parameter	Description	$CHCl_3$	CCl_4	DMF
k_{dam}	Proportionality constant relating rate of metabolism to damage (damage units/mg/l)	1[a]	**8.739**[b]	**0.5255**[c]
k_{dam}	Maximum repair capacity (damage units/h)	95.3[a]	95.3[a]	95.3[a]
k_1	Half-maximal damage (damage units)	186.1[a]	186.1[a]	186.1[a]
β_{ctrl}	Cell death rate of control liver (h^{-1})	7.7×10^{-5}[d]	7.7×10^{-5}[d]	7.7×10^{-5}[d]
k_1	Proportionality between amount of damage and death rate ([damage units $\times$ h]$^{-1}$)	1.0×10^{-6}[a]	1.0×10^{-6}[a]	1.0×10^{-6}[a]
Th	Threshold level of damage (damage units)	6.97[a]	6.97[a]	6.97[a]
α_{ctrl}	Cell division rate of control liver (h^{-1})	7.7×10^{-5}[e]	7.7×10^{-5}[e]	7.7×10^{-5}[e]
N_{ctrl}	Number of cells in control liver	1.69×10^{8}[f]	1.69×10^{8}[f]	1.69×10^{8}[f]
α_{max}	Maximum possible division rate (h^{-1})	0.045[g]	0.045[g]	0.045[g]

[a]Tan *et al.* (2003).
[b]Optimized to data (Benson and Springer, 1999).
[c]Optimized to data (Senoh *et al.*, 2004).
[d]Set equal to α_{ctrl} to ensure no change in liver size.
[e]Calculated from the control labeling index of Larson *et al.* (1996).
[f]Weibel *et al.* (1969).
[g]Conolly *et al.* (2003) and Liao *et al.* (2007).

$$\frac{dP_1(s,T)}{ds} = \alpha_1(T-s)P_1^2(s,T) + \beta_1(T-s) - [\alpha_1(T-s) + \beta_1(T-s) + \mu_1(T-s)]P_1(s,T), \quad (4)$$

with initial conditions

$$P_N(0,T) = 1, \quad P_1(0,T) = 1,$$

$P_N(s,T)$ represented the probability that no progeny of a normal cell at time $(T-s)$ became malignant by time T. Similarly, $P_1(s,T)$ was the probability that no progeny of an initiated cell became malignant by time T. Detailed derivation of Equations 3 and 4 was presented in Portier *et al.* (1996, 2000).

As in previous papers using the clonal growth model, we assumed that once a malignant cell was generated, its growth was deterministic and it became a detectable tumor after a certain (constant) period of time. A delay parameter, D, was used to translate predictions along the time axis. Thus, the cumulative probability that a tumor was present at age T was computed as follows:

$$P(T \le t + D) = 1 - (P_N(T,T))^{N_0}, \quad (5)$$

where N_0 equaled the number of normal cells at time 0.

Parameter Estimation

Unless otherwise stated, all optimal parameters were identified using MATLAB's fminsearchbnd command (available at www.matlabcentral.com). This command is an implementation of the Nelder-Meade simplex algorithm, which allows the user to specify lower and upper bounds for the possible parameter space. fminsearchbnd was used to find the parameters that minimize the following ordinary least squares (OLS) cost function (Sheiner and Beal, 1985),

$$J = \sum_{i=1}^{N} |f(T;d_i;q) - z_i|^2, \quad (6)$$

where $f(T;d_i;q)$ is the model approximation at the final time T, with the ith dose (d_i) and the parameter set q, and z_i represents the data for dose d_i.

For each of the three chemicals, the optimization routine was run with a variety of initial iterates to verify that the identified optimal parameters were not the product of a local minimum. For the optimal parameters reported for $CHCl_3$ and CCl_4, each initial iterate resulted in the reported optimal value. However, the optimization routine for DMF did not identify a unique set of optimal parameters from the varied initial iterates. This was likely because we attempted to identify both the k_{dam} and the *BD* parameter values using tumor incidence data, whereas we only identified the *BD* parameter value for the other two chemicals. We report an optimal parameter set for DMF that produced the lowest cost function value. It should be noted, however, that several parameter combinations (optimal parameters identified *via* other initial iterates) resulted in similar cost function values.

RESULTS

Chloroform

Parameters for the cytotoxicity portion of the model for $CHCl_3$ were taken from previously published models (Liao *et al.*, 2007; Tan *et al.*, 2003). The model was then used to predict hepatic labeling indices of female B6C3F1 mice. A comparison of the ensuing simulations with published labeling index data (Larson *et al.*, 1996) shows that the model simulations are consistent with the data, as depicted in Figure 2.

The parameters for the clonal growth portion of the $CHCl_3$ model are reported in Table 3. Because we could not uniquely identify both the growth advantage and the mutation probability parameters with our limited data set, the mutation parameter, μ_N, was set at an estimated 2.6×10^{-9} (1/h). This value fell within a range of reported values (Ro and Rannala, 2007; Tsuzuki *et al.*, 2001) and allowed for an adequate fit to the control data. Then, the initiated cells' death rate reduction parameter *BD* was optimized to tumor incidence data presented by Yamamoto *et al.* (2002). The optimal value of *BD* was found to be 0.731, resulting in an OLS cost function value of 11.63. Time course simulations of tumor incidences for mice subjected to 0, 5, 30, or 90 ppm of $CHCl_3$ for 6 h/day, 5 days/

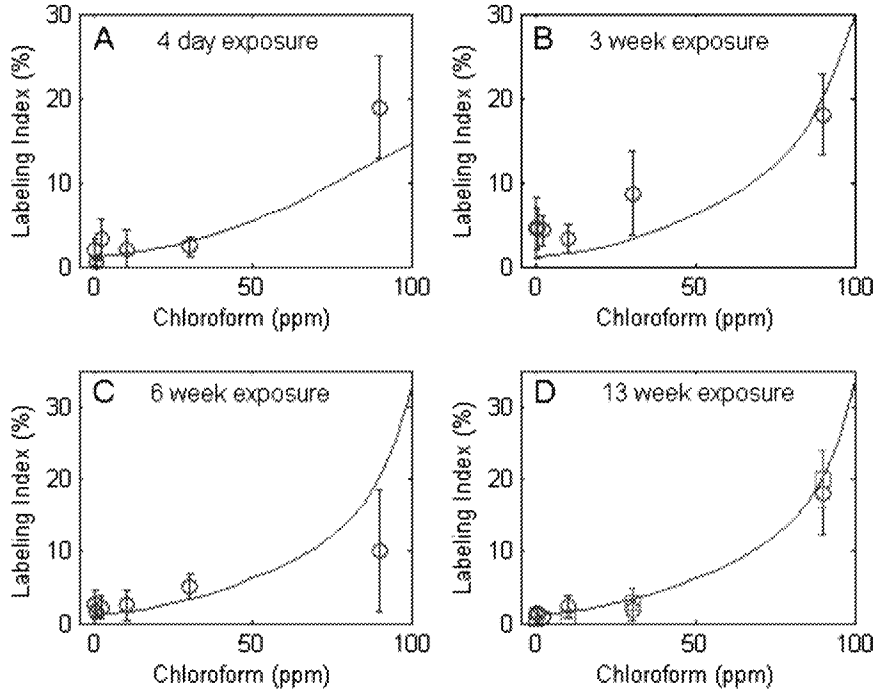

FIG. 2. Hepatocyte labeling indices in female B6C3F1 mice exposed to chloroform vapors. Model simulation (solid lines) and experimental data (open circles) from Larson *et al.* (1996) are presented for mice that were exposed to $CHCl_3$ 6 h/day, 7 days/week, for (A) 4 days, (B) 3 weeks, (C) 6 weeks, and (D) 13 weeks. Open squares in (D) represent the 13-week data from Constan *et al.* (2002) to which the Tan *et al.* (2003) model was originally parameterized. Data points are means, with error bars representing SD, as computed in the original studies.

week, for 104 weeks are shown in comparison to the tumor incidence data in Figure 3. Model estimates for the 0 and 5 ppm doses were slightly higher than the data, while estimates for the 30 ppm dose underpredicted. The model estimate for the highest dose (90 ppm) is consistent with the published data. It should be noted that without a more complete data set (i.e., time-to-tumor data), it was not possible to determine the delay parameter, D, thus it was set equal to 6982 (h) as reported by Conolly *et al.* (2003). Effect of the choice of this parameter was further investigated using several possible values. Results of this analysis showed that although the value of D slightly impacted individual estimation of the clonal growth model parameters, numerical trends remained similar, enabling conclusions of the overall model behavior across chemicals. Results from this investigation are presented in Supplementary table 1.

Carbon Tetrachloride

With the exception of the k_{dam} parameter, all parameter values for the cytotoxicity portion of the CCl_4 model were set equal to the values used for the $CHCl_3$ model. The biological representations of all parameters except k_{dam} are related to dynamic processes within the cell, which are assumed not to

TABLE 3
Parameter Values for the Two-Stage Clonal Growth Model (optimized values are in bold)

Parameter	Description	$CHCl_3$	CCl_4	DMF
μ_N	Probability of a normal cell attaining a mutation	2.6×10^{-9a}	2.6×10^{-9a}	2.6×10^{-9a}
μ_N	Probability of an initiated cell attaining a mutation	2.6×10^{-9b}	2.6×10^{-9b}	2.6×10^{-9b}
BD	Death rate reduction for initiated cells	**0.731**[c]	**0.516**[d]	**0.466**[e]
GA	Proliferation rate increase for initiated cells	**1.275**[c]	**1.502**[d]	**1.539**[e]

[a]Fixed within a range of reported values (Ro and Rannala, 2007; Tsuzuki *et al.*, 2001) and optimized to control.
[b]Set equal to μ_N.
[c]Optimized to tumor incidence data (Yamamoto *et al.*, 2002).
[d]Optimized to tumor incidence data (Nagano *et al.*, 2007).
[e]Optimized to tumor incidence data (Senoh *et al.*, 2004).

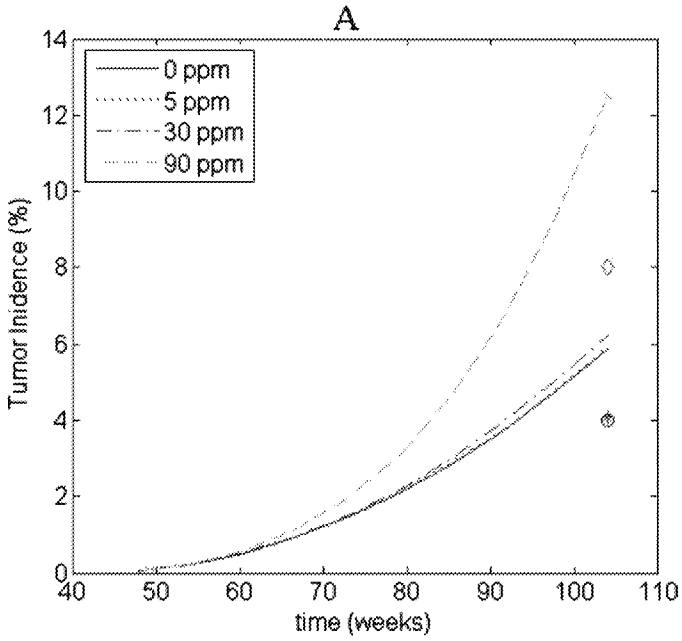

FIG. 3. (A) Time course hepatic tumor incidence simulations compared to hepatic tumor incidence data from female B6C3F1 mice exposed to chloroform vapor for 104 weeks (Yamamoto *et al.*, 2002). The following concentrations of chloroform were examined: 0 ppm (solid line, open circle), 5 ppm (dotted line, asterisk), 30 ppm (dash-dot line, open diamond), and 90 ppm (dashed line, x).

vary with chemical. An optimal value for k_{dam} of 8.739 damage units/mg/l was found using labeling index data reported by Benson and Springer (1999). The optimized simulations are presented in comparison to the data in Figure 4. The simulated labeling indices seem consistent with the data, with the exception of the highest dose (100 ppm) during the 1-week exposure, which underpredicts the reported labeling index.

The clonal growth portion of the CCl_4 model was parameterized using tumor incidence data from female B6C3F1 mice exposed *via* inhalation to 0, 5, 25, and 125 ppm of CCl_4 for 6 h/day, 5 days/week, for 104 weeks (Nagano *et al.*, 2007). Values for μ_N and D that were used in the $CHCl_3$ model were also used for CCl_4. Thus, the only CCl_4 parameter that was identified *via* optimization was *BD*, and its optimal value was 0.516 (unitless). This resulted in an OLS cost function value of 99.57. Model predictions of tumor incidences for CCl_4 are illustrated in Figure 5. The model prediction was lower than the reported tumor incidence for 5 ppm of CCl_4, but predictions for the other three doses provided close fit to their corresponding data values.

Nagano *et al.* (2007) showed that although tumor incidence levels were increased at the lowest dose (5 ppm) of CCl_4, cellular proliferation levels did not significantly increase as they did at higher exposure levels. Because model simulations in Figure 5 are based on cytotoxicity and cellular proliferation as sole mechanisms for tumor incidences MOA of CCl_4, failure of the model to simulate results at the 5 ppm dose of CCl_4 is expected. At this dose, mechanisms other than cytotoxicity/increased cellular proliferation that were not included in the model may be important (Nagano *et al.*, 2007).

Dimethylformamide

With no published PBPK model for DMF, we first constructed and parameterized a model to predict the metabolism rate of DMF in the liver. We employed the same general model structure that was used for the $CHCl_3$ and CCl_4 PBPK models (Equations A1–A9). However, since the available data for DMF included plasma concentrations and amounts of DMF excreted in the urine during a 24-h period (Hundley *et al.*, 1993), a few minor modifications were necessary. Urinary excretion was included in the model as clearance from the kidney using a first order rate constant, k_u (Equation A5).

Because the available pharmacokinetic data for DMF included concentration in plasma, we modified the PBPK model to evaluate plasma concentrations. The concentration of chemical in the blood (C_B) as a function of the concentration in the plasma (C_P) and the concentration in the red blood cells (C_{RBC}) can be written as follows (Laplanche *et al.*, 2007):

$$C_B = (1 - H) \cdot C_P + H \cdot C_{RBC}. \quad (7)$$

Assuming that binding between DMF and the red blood cells is insignificant ($C_{RBC} \approx 0$), then $C_P \approx \frac{C_B}{1-H}$, where H represents the hematocrit of the mouse (we used a value of 45%, as reported in Trune *et al.*, 2006). Finally, since blood is divided between the arterial and venous compartments at a volumetric ratio of 1:3 (Kohn, 1997), plasma concentrations were computed for the DMF model using the following equation:

$$C_P = \frac{0.75 \cdot C_V + 0.25 \cdot C_A}{1 - H}, \quad (8)$$

where C_V is the concentration of DMF in the venous blood and C_A is the concentration of DMF in the arterial blood.

We determined optimal values for the maximal metabolism rate (V_{max}, 1.085 mg/h) and the urinary excretion rate (k_u, 8.5×10^{-5} l/h) parameters to the time course DMF plasma concentration and urinary excretion data reported by Hundley *et al.* (1993) for mice exposed to 250 or 500 ppm DMF *via* inhalation for 6 h. A comparison of the PBPK model simulations with the published data are shown in Figure 6 (plasma concentration) and Figure 7 (urinary excretion). The model simulations provide an adequate fit to the plasma concentration data with a slight overprediction for the 250 ppm data set. Model simulations for the urinary excretion were lower than the reported values for the 250 ppm exposure and higher than the reported 500 ppm exposure values.

The chemical-specific parameters for the cytotoxicity and clonal growth portions of the DMF model were optimized to published tumor incidences after a 104-week study (Senoh *et al.*, 2004). Female B6C3F1 mice were exposed *via* inhalation to 0, 200, 400, and 800 ppm of DMF for 6 h/day, 5 days/week, for 104 weeks. Optimal values were

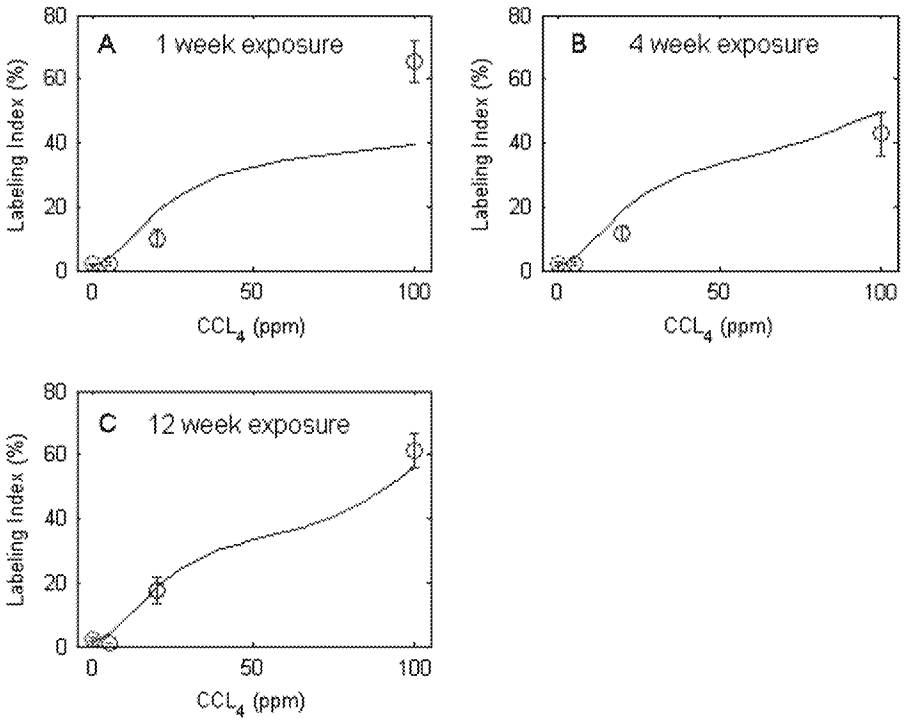

FIG. 4. Hepatocyte labeling indices in female B6C3F1 mice exposed to CCl_4 vapors. Model simulation (solid lines) and experimental data (open circles) from Benson and Springer (1999) are presented for mice that were exposed to CCl_4 for 6 h/day, 5 days/week, for (A) 1 week, (B) 4 weeks, and (C) 12 weeks. Data points are means, with error bars representing SD, as computed in the original studies.

simultaneously identified for k_{dam} (0.5255 damage units/mg/l) and *BD* (0.466 unitless), yielding an OLS cost function value of 4.01. Figure 8 depicts the resulting time course simulation of tumor incidence due to dimethylformamide exposure. Model simulations accurately predict the reported tumor incidences for all exposure levels of DMF.

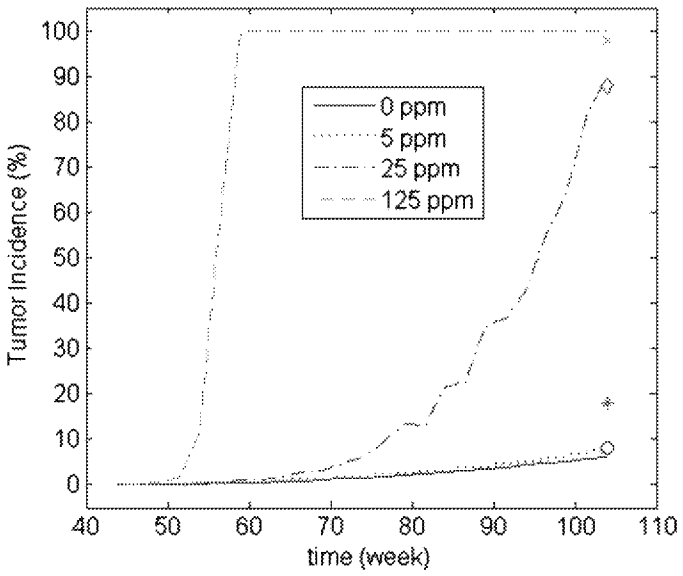

FIG. 5. (A) Time course hepatic tumor incidence simulations compared to hepatic tumor incidence data from female B6C3F1 mice exposed to CCl_4 vapor for 104 weeks (Nagano *et al.*, 2007). The following concentrations of CCl_4 were examined: 0 ppm (solid line, open circle), 5 ppm (dotted line, asterisk), 25 ppm (dash-dot line, open diamond), and 125 ppm (dashed line, x).

DISCUSSION

The purpose of the modeling effort in this manuscript was to develop a generalized computational model incorporating key events in a cytotoxic MOA for tumorgenicity and to test if the proposed hypothesis of cytotoxicity leading to regenerative proliferation and tumor formation is supported for all chemicals examined. Once chemical-specific processes cause cytotoxicity, the magnitude of resulting regenerative proliferation and tumors is not expected to be chemical dependent but directly related to the hypothesized key events leading to tumor formation. Although it is critically important to evaluate the contribution of other MOAs to the tumorigenic response, BBDR efforts as described here can only test MOA hypothesis for which there exists empirical data, it cannot predict an alternative MOA. For this reason, only the parameters discussed below were explored as they relate to the cytotoxic MOA. If additional data were available to characterize other key events (e.g., genotoxicity, epigenetic events, etc.) within alternative MOAs, additional parameters could be explored in a similar fashion.

Overall BBDR model consisted of pharmacokinetic and PD components. Pharmacokinetic parameters varied between the

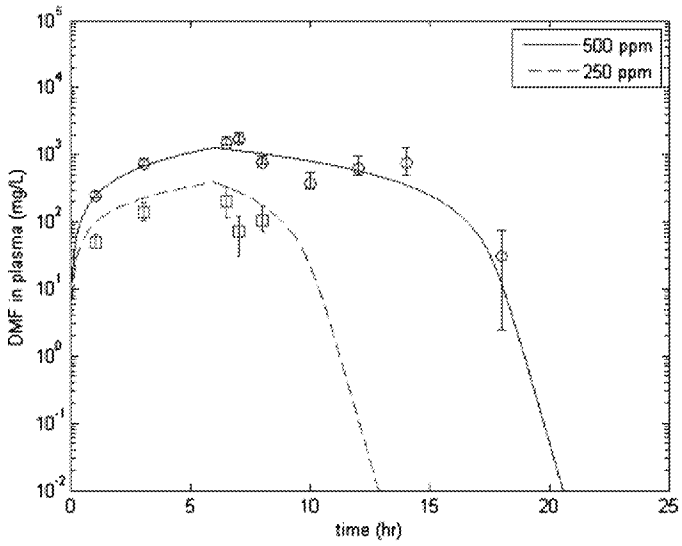

FIG. 6. Model predictions (lines) of DMF plasma concentrations (symbols) determined by Hundley *et al.* (1993) for male B6C3F1 mice following a single 6-h exposure to 250 ppm (solid line, circle) or 500 ppm (dashed line, square) DMF.

three tested chemicals as expected. Two parameters related to the PD section of the model (k_{dam} and BD) were optimized using labeling indices and tumor incidences data for each chemical.

Model Optimization of the First Order Cellular Injury Rate Constant (k_{dam})

Labeling index data can be used to infer the amount of regenerative cellular proliferation in the liver after exposure to a chemical. The labeling index provides an estimate of the percentage of hepatocytes that were in S-phase during the period

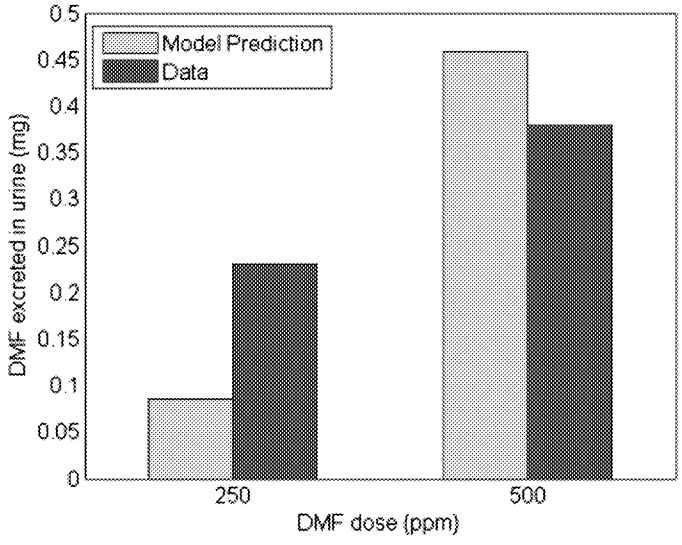

FIG. 7. PBPK model prediction of DMF excreted in urine by male B6C3F1 mice following a single 6-h exposure to 250 or 500 ppm compared with data (Hundley *et al.*, 1993).

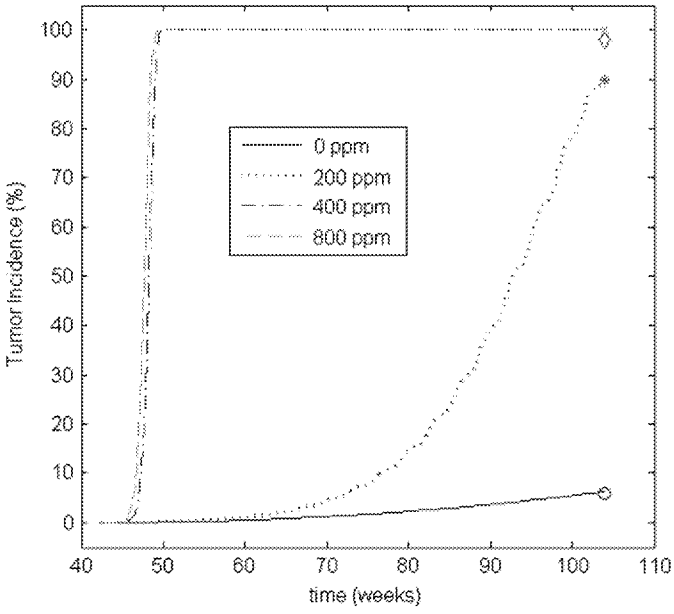

FIG. 8. (A) Time course hepatic tumor incidence simulations compared to hepatic tumor incidence data from female B6C3F1 mice exposed to DMF vapor for 104 weeks (Senoh *et al.*, 2004). Hepatic tumor incidence was estimated by the model and compared to data for animals exposed to: 0 ppm (solid line, open circle), 200 ppm (dotted line, asterisk), 400 ppm (dash-dot line, open diamond), and 800 ppm (dashed line, x).

of exposure to a DNA precursor–labeling agent, such as BrdU. Hepatic labeling indices for various doses of $CHCl_3$ and CCl_4 were reported by Larson *et al.* (1996) and Benson and Springer (1999), respectively. Table 4 presents a brief chemical comparison of labeling index, showing the dose for each chemical that resulted in an 18% fixed labeling index and the corresponding tumor incidences.

Laboratory experiments showed that doses of 90 ppm for $CHCl_3$ (Larson *et al.*, 1996) and 25 ppm for CCl_4 (Benson and Springer, 1999) result in a labeling index of 18%. Utilizing the cytotoxicity model for DMF, we estimated that a dose of approximately 265 ppm of DMF would correspond to an 18% labeling index. Each chemical has a different dose that leads to a labeling index of 18%, which implies that the chemicals vary in their cytotoxic potency. As such, some portion of the parameter space for the cytotoxicity model must differ among the various chemicals; therefore, we varied the parameter k_{dam} by chemical. Because k_{dam} is a proportionality constant that relates the rate of chemical metabolism to the amount of damage attained, it may also be considered a measure of cytotoxic potency. For a chemical with a higher k_{dam} value, less chemical metabolism (e.g., lower doses or slower metabolism rate) would produce a regenerative proliferation rate equal to that of a chemical with a lower k_{dam} value and faster metabolism rate. This suggests that chemicals with higher k_{dam} values are more cytotoxic.

Thus, using k_{dam} values as an indicator of toxicity, CCl_4 (k_{dam} = 8.739 damage units/mg/l) is the most toxic of the chemicals examined, followed by chloroform (k_{dam} = 1 damage

TABLE 4
Chemical Comparison of Labeling Index and Tumor Incidence Data

	$CHCl_3$	CCl_4	DMF
Dose (ppm)	90[a,b]	25[c,d]	265[e]
Labeling index (%)	18[a]	18[c]	18[e]
Tumor incidence (%)	12[b]	85[d]	100[e]

[a]Larson *et al.* (1996).
[b]Yamamoto *et al.* (2002).
[c]Benson and Springer (1999).
[d]Nagano *et al.* (2007).
[e]Model estimated.

units/mg/l). DMF appears to be the least potent (k_{dam} = 0.5255 damage units/mg/l). This observation is also reflected in Table 4, with CCl_4 requiring the lowest dose (25 ppm) and DMF requiring the highest dose (265 ppm) to result in a labeling index of 18%.

We further examined the relative hepatotoxicity by considering sorbitol dehydrogenase (SDH) activity. SDH is an enzyme that is highly sensitive for liver cell necrosis (Korsrud *et al.*, 1972, 1973). As such, SDH activity may serve as a marker for cytotoxicity. Lundberg *et al.* (1986) presented a comparison of SDH activity in rats after an ip injection of several different industrial solvents. Using their reported levels for CCl_4, $CHCl_3$, and DMF, we formulated linear equations to relate the administered dose to the SDH activity levels and calculated the slope of the lines (Table 5). In order to compare these slopes with the chemical-specific k_{dam} parameters, each slope was normalized to the slope for $CHCl_3$. This resulted in normalized slopes of 14.68, 1, and 0.5428 for CCl_4, $CHCl_3$, and DMF, respectively. These values compare favorably to the optimal k_{dam} values that were estimated from model comparisons to labeling index data. These results suggest that incorporating a measurable marker of damage (as in k_{dam}), such as SDH, into future modeling efforts is feasible.

Model Estimation of the Death Rate Reduction Parameter (BD)

The clonal growth portion of the model relates cellular proliferation to tumor formation. The data presented in Table 4 show for three chemicals that different tumor incidences result from an 18% labeling index. An 18% labeling index for $CHCl_3$ corresponds the lowest tumor incidence (12%), and DMF results in the highest tumor incidence (predicted to be 100%). This is also reflected in the optimal values of the death rate reduction parameter (*BD*). Estimated parameter values for DMF and CCl_4 suggest that the death rate for the population of initiated cells is reduced by approximately 50% (*BD* = 0.466 and 0.516, respectively), while the estimation for $CHCl_3$ predicts a lower 27% (*BD* = 0.731) reduction in the initiated cells' death rate. There is supporting evidence in literature indicating a unique impact for $CHCl_3$ in conjunction with other carcinogenic compound regarding the formation of liver tumors. Administration of $CHCl_3$ in drinking water inhibited liver and lung tumors of ethylnitrosourea-imitated mice (Pereira *et al.*, 1985). Also, $CHCl_3$ was shown to inhibit hypomethylation and increased messenger RNA expression of the c-myc gene and the production of liver tumors by dichloroacetic acid in mice (Pereira *et al.*, 2001).

TABLE 5
Comparison of SDH and the Parameter k_{dam}

	Linear slope (SDH to dose)	Ratio to $CHCl_3$	k_{dam}
$CHCl_3$	0.2074	1	1
CCl_4	3.044	14.68	8.739
DMF	0.1126	0.5428	0.5255

The hypothesis that cytotoxicity leads to regenerative proliferation and tumors implies that these relationships are independent of chemical. That is, a given level of cytotoxicity will lead to the same level of regenerative proliferation and tumor response regardless of which chemical produced the cytotoxicity. This hypothesis was evaluated by developing a BBDR that described the relationship between cytotoxicity, regenerative proliferation and tumor response. This model was applied to data sets for $CHCl_3$, CCl_4, and DMF. The model adequately described the data for each chemical, although *BD* was chemical specific. This implies that additional key events beyond cytotoxicity leading to cellular proliferation are needed to explain differences in tumor incidences across chemicals sharing the same MOA. For example, mechanisms by which chemicals may interact with initiated cells may be crucial in subsequent tumor formation. Across all three chemicals, the results of the modeling exercises in this paper suggest that without a growth advantage given to initiated cells, background mutation rates and increased cellular proliferation are not quantitatively enough to cause tumors. Additionally, mechanisms that allow for initiated cells' growth advantage, as well as their rates, may vary across chemicals. Therefore, cytotoxicity alone as manifested by increased proliferation rate in response to cellular injury without considering dynamics of initiated cells is not sufficient as a MOA to quantitatively account for tumor incidences across these three chemicals (i.e., $CHCl_3$, CCl_4, and DMF).

An Alternative Formulation of the Model

As previously stated, the growth advantage present within the initiated cell population, which is necessary to induce tumor incidences, can be achieved computationally by reducing the death rate of the initiated cells or by increasing the proliferation rate of the initiated cells. The results presented within this manuscript have been generated using the former mechanism. However, a simple change to the model will allow the investigation of the latter mechanism.

A growth advantage which occurs due to an increased proliferation rate can be considered by replacing the death and division rates of the initiated cells (Equations 1 and 2) with the following:

$$\alpha_I(t) = \begin{cases} \alpha_N(t) & \text{if dose} = 0 \\ \alpha_N(t) \cdot GA & \text{if dose} > 0 \end{cases} \quad (9)$$

$$\beta_I(t) = \beta_N(t)\,, \quad (10)$$

where the *GA* parameter represents the increase of the initiated cells' proliferation rate over that of the normal cells (i.e., $GA > 1$).

With this revised formulation of the model, we again utilized the optimization routine to identify optimal values for the *GA* parameter for each chemical. The same results which have been presented are yielded for $CHCl_3$ when $GA = 1.275$ (a 27% increase), for CCl_4 when $GA = 1.502$ (a 50% increase), and for DMF when $GA = 1.539$ (a 53% increase). Notice that, as with the previous formulation using a decreased death rate, the parameters for CCl_4 and DMF are remarkably similar, while the parameter for $CHCl_3$ differs by more than 20%. These parameter values are compared to the previous results in Table 3.

Future Directions for Model Improvement

The overall model consisted of three submodels: PBPK to estimate rate of metabolism, cytotoxicity to estimate increased proliferation rate, and a two-stage clonal model to estimate tumor incidences. The overall model presented in this paper is unique from previous tumor modeling efforts because it connects tumor incidence estimates with rates of metabolism and measures of cytotoxicity. Data used for the PBPK and cyotoxicity components of the models were either obtained or recalculated from literature. The parameters for the two-stage clonal growth model were estimated using tumor incidences as they are reported in literature. The lack of time-to-tumor data is a source of uncertainty for the predicted shape of the model-generated temporal relationship of the tumor incidence. For instance, when examining the tumor incidence curves for CCl_4 and DMF, especially at the higher doses (Figs. 5 and 8), the model predicted an initial sharp increase in tumor incidences. The tumor incidence reaches 100% very quickly (after 45–60 weeks). This would imply that either the animals develop and live with hepatic tumors for 40+ weeks or the animals die with hepatic tumors before the conclusion of the study. The accuracy of the tumor incidence trajectories could be better evaluated if a more complete data set, which included time-to-tumor data, is collected. However, in the absence of this data, models can be developed based on available information from literature to identify as many parameters as possible. These literature-based models can be a valuable tool to numerically test MOA applicability in comparison to experimental data (upon which MOA are initially hypothesized) and identity data gaps.

In the two-stage clonal growth model presented here, the parameters for the probability of a normal cell attaining a mutation (μ_N), the probability of an initiated cell attaining a mutation (μ_I), and the death rate reduction constant for initiated cells (*BD*) are needed. As was shown in Table 3, the magnitude of μ_N was fixed using a range of observed values in literature (Ro and Rannala, 2007; Tsuzuki *et al.*, 2001) and optimization to control data. The value of μ_I was set equal to μ_N as usually done for this type of modeling, specifically under the assumptions that chemicals under investigation did not show sufficient evidence in literature to produce mutations above background. Therefore, the only parameter in the two-stage clonal growth model utilized in this study that was fit to dose-response data is *BD*. Further confidence on the estimate of this parameter was based on using several doses for each chemical's tumor incidence dose-response data. Our estimate for the delay parameter was based on an earlier value obtained from the formaldehyde study because it incorporated time-to-tumor data in nasal tissues. Uncertainty may exist due to the possibility of differences between delay parameters between tissues (nasal vs. liver), for which data to determine tissue-specific parameters may provide improvements to the existing model. Additionally, further experimental data utilizing time-to-tumor data and estimates of proliferation and death rates within foci for the three tested chemicals in this study can be useful in verifying model parameterization and findings.

Benefits to Risk Assessment

The benefits to human health risk assessment from this and other BBDR models are directly dependent upon existing and future empirical data characterizing the kinetics and health effects of environmental pollutants. Mathematical models that provide reasonable predictions of induced adverse health effects based on key events of a MOA provide the current utility of (1) qualitative weight of evidence contributions for compounds hypothesized to work through this MOA, (2) prioritization/screening tool for compounds with unknown toxicity, and (3) specific research needs (e.g., empirical data, assay specificity). Additionally, if a compound is hypothesized to work through a MOA and the available data do not provide a reasonable fit, it may indicate that other additional key events or MOA(s) contribute to the overall toxicity.

A critical point made by the NRC (2007) is that quantitative modeling efforts of this type must be initiated broadly to achieve scientific milestones within a reasonable period of time. Utilizing BBDR models for risk assessment has been previously described (Andersen *et al.*, 2002; Edwards and Preston, 2008). Our BBDR model provided adequate fit to data when cytotoxicity as MOA for tumorigenesis was considered for each chemical alone. However, comparison of the model parameters (specifically *BD*) obtained from fitting model simulations to data for all three chemicals suggests that cytotoxicity, as presented by cell injury leading to increased cellular proliferation and tumor formation, oversimplifies several possible key steps that may take place *in vivo* as was shown in the case of $CHCl_3$.

Another value of this type of modeling effort is to identify critical data needs for carcinogenic risk assessment. For example, the model suggests a need to identify steps beyond

cellular proliferation to explain differences in tumor incidences between $CHCl_3$ and the other two chemicals when all produce similar cellular proliferation rates (Table 4).

The present study provides an example of the utility of BBDR modeling in testing a unified MOA across chemicals. While the present model requires additional verification across larger sets of chemicals, it is at least informative for the chemicals tested here. Results from the model suggested that, for $CHCl_3$, CCl_4, and DMF, cytotoxicity as described by single events for injury, cellular proliferation, and tumor formation may be an oversimplification of other mechanisms, key events, or MOAs that may exist.

SUPPLEMENTARY DATA

Supplementary data are available online at http://toxsci.oxfordjournals.org/.

ACKNOWLEDGMENTS

This manuscript has been reviewed in accordance with the policy of the National Health and Environmental Effects Research Laboratory, U.S. Environmental Protection Agency, and approved for publication. Approval does not signify that the contents necessarily reflect the views and policies of the Agency nor does mention of trade names or commercial products constitute endorsement or recommendation for use. The authors would like to thank Dr Christopher Portier for valuable insight into growth modeling. Additionally, the authors also express gratitude to Dr Marina Evans, Dr Woodrow Setzer, Dr John Wambaugh, Dr Eva McLanahan, Dr Andrew Rooney, and Dr John Vandenberg for helpful comments during the preparation of this manuscript.

APPENDIX

$$\frac{dC_{CH}}{dt} = \frac{1}{V_{CH}}\left(Q_{CH}\left(\text{dose} - C_{CH}\right) + Q_P\left(\frac{C_A}{P_B} - C_{CH}\right)\right) - k_{loss}C_{CH} \quad \text{(A1)}$$

$$\frac{dC_R}{dt} = \frac{Q_R}{V_R}\left(C_A - \frac{C_R}{P_R}\right) \quad \text{(A2)}$$

$$\frac{dC_S}{dt} = \frac{Q_S}{V_S}\left(C_A - \frac{C_S}{P_S}\right) \quad \text{(A3)}$$

$$\frac{dC_F}{dt} = \frac{Q_F}{V_F}\left(C_A - \frac{C_F}{P_F}\right) \quad \text{(A4)}$$

$$\frac{dC_K}{dt} = \frac{1}{V_K}\left(Q_K\left(C_A - \frac{C_K}{P_K}\right) - \frac{V_{maxK}C_K}{K_m + C_K} - k_U C_K\right) \quad \text{(A5)}$$

$$\frac{dC_{LI}}{dt} = \frac{1}{V_{LI}}\left(Q_{LI}\left(C_A - \frac{C_{LI}}{P_{LI}}\right) - \frac{V_{max}C_{LI}}{K_m + C_{LI}}\right) \quad \text{(A6)}$$

$$C_V = \frac{1}{Q_C}\left(Q_R\frac{C_R}{P_R} + Q_S\frac{C_S}{P_S} + Q_F\frac{C_F}{P_F} + Q_K\frac{C_K}{P_K} + Q_{LI}\frac{C_{LI}}{P_{LI}}\right) \quad \text{(A7)}$$

$$C_A = \frac{Q_P C_{CH} + Q_C C_V}{Q_P/P_B + Q_C} \quad \text{(A8)}$$

$$V_{maxK} = A \cdot V_K \frac{V_{max}}{V_{LI}} \quad \text{(A9)}$$

$$\frac{dA_{dam}}{dt} = k_{dam}\frac{V_{max}C_{LI}}{V_{LI}(K_m + C_{LI})} - \frac{k_{max}A_{dam}}{k_1 + A_{dam}} \quad \text{(A10)}$$

$$\frac{dN}{dt} = N\left(\alpha_N - \beta_N\right) \quad \text{(A11)}$$

$$\frac{dN_{labeled}}{dt} = \alpha_N(2N - N_{labeled}) - \beta_N N_{labeled} \quad \text{(A12)}$$

$$\alpha_N = \alpha_{ctrl}\left(\frac{N}{N_{ctrl}}\right) + \alpha_{max}\left(1 - \frac{N}{N_{ctrl}}\right) \quad \text{(A13)}$$

$$\beta_N = \begin{cases} \beta_{ctrl} + k_2(A_{dam} - Th) & \text{when } A_{dam} > Th \\ \beta_{ctrl} & \text{when } A_{dam} \le Th \end{cases} \quad \text{(A14)}$$

$$LI = 100\frac{N_{labeled}}{N} \quad \text{(A15)}$$

REFERENCES

Andersen, M. E., and Conolly, R. B. (1998). Mechanistic modeling of rodent liver tumor promotion at low levels of exposure: an example related to dose-response relationships for 2,3,7,8-tetrachlorodibenzo-p-dioxin. *Hum. Exp. Toxicol.* **17,** 683– 690; discussion 701–684, 708–618.

Andersen, M. E., Yang, R. S., French, C. T., Chubb, L. S., and Dennison, J. E. (2002). Molecular circuits, biological switches, and nonlinear dose-response relationships. *Environ. Health Perspect.* **110**(Suppl. 6), 971–978.

Benson, J. M., and Springer, D. L. (1999). Improved risk estimates for carbon tetrachloride. Final report. Technical Report DE-FC04-96AL76406. Project No. 54940

Benson, J. M., Tibbetts, B. M., Thrall, K. D., and Springer, D. L. (2001). Uptake, tissue distribution, and fate of inhaled carbon tetrachloride: comparison of rat, mouse, and hamster. *Inhal. Toxicol.* **13,** 207–217.

Bergheim, I., Wolfgarten, E., Bollschweiler, E., Holscher, A. H., Bode, C., and Parlesak, A. (2007). Cytochrome P450 levels are altered in patients with esophageal squamous-cell carcinoma. *World J. Gastroenterol.* **13,** 997–1002.

Branchflower, R. V., Nunn, D. S., Highet, R. J., Smith, J. H., Hook, J. B., and Pohl, L. R. (1984). Nephrotoxicity of chloroform: metabolism to phosgene by the mouse kidney. *Toxicol. Appl. Pharmacol.* **72,** 159–168.

Brown, R. P., Delp, M. D., Lindstedt, S. L., Rhomberg, L. R., and Beliles, R. P. (1997). Physiological parameter values for physiologically based pharmacokinetic models. *Toxicol. Ind. Health* **13,** 407–484.

Cohen, S. M., Ohnishi, T., Arnold, L. L., and Le, X. C. (2007). Arsenic-induced bladder cancer in an animal model. *Toxicol. Appl. Pharmacol.* **222,** 258–263.

Collins, F. S., Gray, G. M., and Bucher, J. R. (2008). Toxicology. Transforming environmental health protection. *Science* **319,** 906–907.

Conolly, R. B., Kimbell, J. S., Janszen, D., Schlosser, P. M., Kalisak, D., Preston, J., and Miller, F. J. (2003). Biologically motivated computational

modeling of formaldehyde carcinogenicity in the F344 rat. *Toxicol. Sci.* **75,** 432–447.

Constan, A. A., Wong, B. A., Everitt, J. I., and Butterworth, B. E. (2002). Chloroform inhalation exposure conditions necessary to initiate liver toxicity in female B6C3F1 mice. *Toxicol. Sci.* **66,** 201–208.

Corley, R. A., Mendrala, A. L., Smith, F. A., Staats, D. A., Gargas, M. L., Conolly, R. B., Andersen, M. E., and Reitz, R. H. (1990). Development of a physiologically based pharmacokinetic model for chloroform. *Toxicol. Appl. Pharmacol.* **103,** 512–527.

Crump, K. S., Subramaniam, R. P., and Van Landingham, C. B. (2005). A numerical solution to the nonhomogeneous two-stage MVK model of cancer. *Risk Anal.* **25,** 921–926.

Edwards, S. W., and Preston, R. J. (2008). Systems biology and mode of action based risk assessment. *Toxicol. Sci.* **106,** 312–318.

Gluck, S. J., Benko, M. H., Hallberg, R. K., and Steele, K. P. (1996). Indirect determination of octanol-water partition coefficients by microemulsion electrokinetic chromatography. *J. Chromatogr. A* **744,** 141–146.

Hard, G. C. (2002). Significance of the renal effects of ethyl benzene in rodents for assessing human carcinogenic risk. *Toxicol. Sci.* **69,** 30–41.

Ho, J. C., Cheung, S. T., Leung, K. L., Ng, I. O., and Fan, S. T. (2004). Decreased expression of cytochrome P450 2E1 is associated with poor prognosis of hepatocellular carcinoma. *Int. J. Cancer* **111,** 494–500.

Holsapple, M. P., Pitot, H. C., Cohen, S. M., Boobis, A. R., Klaunig, J. E., Pastoor, T., Dellarco, V. L., and Dragan, Y. P. (2006). Mode of action in relevance of rodent liver tumors to human cancer risk. *Toxicol. Sci.* **89,** 51–56.

Hundley, S. G., Lieder, P. H., Valentine, R., Malley, L. A., and Kennedy, G. L., Jr. (1993). Dimethylformamide pharmacokinetics following inhalation exposures to rats and mice. *Drug Chem. Toxicol.* **16,** 21– 52; sW.

Kodell, R. L., Young, J. F., Delongchamp, R. R., Turturro, A., Chen, J. J., Gaylor, D. W., Howard, P. C., and Zheng, Q. (2001). A mechanistic approach to modelling the risk of liver tumours in mice exposed to fumonisin B1 in the diet. *Food Addit. Contam.* **18,** 237–253.

Kohn, M. C. (1997). The importance of anatomical realism for validation of physiological models of disposition of inhaled toxicants. *Toxicol. Appl. Pharmacol.* **147,** 448–458.

Korsrud, G. O., Grice, H. C., and McLaughlan, J. M. (1972). Sensitivity of several serum enzymes in detecting carbon tetrachloride-induced liver damage in rats. *Toxicol. Appl. Pharmacol.* **22,** 474–483.

Korsrud, G. O., Grice, H. G., Goodman, T. K., Knipfel, J. E., and McLaughlan, J. M. (1973). Sensitivity of several serum enzymes for the detection of thioacetamide-, dimethylnitrosamine- and diethanolamine-induced liver damage in rats. *Toxicol. Appl. Pharmacol.* **26,** 299–313.

Laplanche, R., Meno-Tetang, G. M., and Kawai, R. (2007). Physiologically based pharmacokinetic (PBPK) modeling of everolimus (RAD001) in rats involving non-linear tissue uptake. *J. Pharmacokinet. Pharmacodyn.* **34,** 373–400.

Larson, J. L., Templin, M. V., Wolf, D. C., Jamison, K. C., Leininger, J. R., Mery, S., Morgan, K. T., Wong, B. A., Conolly, R. B., and Butterworth, B. E. (1996). A 90-day chloroform inhalation study in female and male B6C3F1 mice: implications for cancer risk assessment. *Fundam. Appl. Toxicol.* **30,** 118–137.

Liao, K. H., Tan, Y. M., Conolly, R. B., Borghoff, S. J., Gargas, M. L., Andersen, M. E., and Clewell, H. J., III. (2007). Bayesian estimation of pharmacokinetic and pharmacodynamic parameters in a mode-of-action-based cancer risk assessment for chloroform. *Risk Anal.* **27,** 1535–1551.

Little, M. P., Heidenreich, W. F., Moolgavkar, S. H., Schollnberger, H., and Thomas, D. C. (2008). Systems biological and mechanistic modelling of radiation-induced cancer. *Radiat. Environ. Biophys.* **47,** 39–47.

Lundberg, I., Ekdahl, M., Kronevi, T., Lidums, V., and Lundberg, S. (1986). Relative hepatotoxicity of some industrial solvents after intraperitoneal injection or inhalation exposure in rats. *Environ. Res.* **40,** 411–420.

Manibusan, M. K., Odin, M., and Eastmond, D. A. (2007). Postulated carbon tetrachloride mode of action: a review. *J. Environ. Sci. Health C Environ. Carcinog. Ecotoxicol. Rev.* **25,** 185–209.

Meek, M. E., Bucher, J. R., Cohen, S. M., Dellarco, V., Hill, R. N., Lehman-McKeeman, L. D., Longfellow, D. G., Pastoor, T., Seed, J., and Patton, D. E. (2003). A framework for human relevance analysis of information on carcinogenic modes of action. *Crit. Rev. Toxicol.* **33,** 591–653.

Moser, G. J., Foley, J., Burnett, M., Goldsworthy, T. L., and Maronpot, R. (2009). Furan-induced dose-response relationships for liver cytotoxicity, cell proliferation, and tumorigenicity (furan-induced liver tumorigenicity). *Exp. Toxicol. Pathol.* **61,** 101–111.

Mraz, J., Jheeta, P., Gescher, A., Hyland, R., Thummel, K., and Threadgill, M. D. (1993). Investigation of the mechanistic basis of N, N-dimethylformamide toxicity. Metabolism of N, N-dimethylformamide and its deuterated isotopomers by cytochrome P450 2E1. *Chem. Res. Toxicol.* **6,** 197–207.

Nagano, K., Sasaki, T., Umeda, Y., Nishizawa, T., Ikawa, N., Ohbayashi, H., Arito, H., Yamamoto, S., and Fukushima, S. (2007). Inhalation carcinogenicity and chronic toxicity of carbon tetrachloride in rats and mice. *Inhal. Toxicol.* **19,** 1089–1103.

National Research Council (NRC). (2007). *Toxicity Testing in the 21st Century: A Vision and a Strategy.* National Academies Press, Washington, DC.

Ohbayashi, H., Yamazaki, K., Aiso, S., Nagano, K., Fukushima, S., and Ohta, H. (2008). Enhanced proliferative response of hepatocytes to combined inhalation and oral exposures to N, N-dimethylformamide in male rats. *J. Toxicol. Sci.* **33,** 327–338.

Pereira, M. A., Knutsen, G. L., and Herren-Freund, S. L. (1985). Effect of subsequent treatment of chloroform or phenobarbital on the incidence of liver and lung tumors initiated by ethylnitrosourea in 15 day old mice. *Carcinogenesis* **6,** 203–207.

Pereira, M. A., Kramer, P. M., Conran, P. B., and Tao, L. (2001). Effect of chloroform on dichloroacetic acid and trichloroacetic acid-induced hypomethylation and expression of the c-myc gene and on their promotion of liver and kidney tumors in mice. *Carcinogenesis* **22,** 1511–1519.

Portier, C. J., Kopp-Schneider, A., and Sherman, C. D. (1996). Calculating tumor incidence rates in stochastic models of carcinogenesis. *Math. Biosci.* **135,** 129–146.

Portier, C. J., Sherman, C. D., and Kopp-Schneider, A. (2000). Multistage, stochastic models of the cancer process: a general theory for calculating tumor incidence. *Stoch. Environ. Res. Risk Assess.* **14,** 173–179.

Poulin, P., and Krishnan, K. (1995). An algorithm for predicting tissue: blood partition coefficients of organic chemicals from n-octanol: water partition coefficient data. *J. Toxicol. Environ. Health* **46,** 117–129.

Ramsey, J. C., and Andersen, M. E. (1984). A physiologically based description of the inhalation pharmacokinetics of styrene in rats and humans. *Toxicol. Appl. Pharmacol.* **73,** 159–175.

Ro, S., and Rannala, B. (2007). Inferring somatic mutation rates using the stop-enhanced green fluorescent protein mouse. *Genetics* **177,** 9–16.

Senoh, H., Aiso, S., Arito, H., Nishizawa, T., Nagano, K., Yamamoto, S., and Matsushima, T. (2004). Carcinogenicity and chronic toxicity after inhalation exposure of rats and mice to N, N-dimethylformamide. *J. Occup. Health* **46,** 429–439.

Sheiner, L. B., and Beal, S. L. (1985). Pharmacokinetic parameter estimates from several least squares procedures: superiority of extended least squares. *J. Pharmacokinet. Biopharm.* **13,** 185–201.

Slikker, W., Jr, Andersen, M. E., Bogdanffy, M. S., Bus, J. S., Cohen, S. D., Conolly, R. B., David, R. M., Doerrer, N. G., Dorman, D. C., Gaylor, D. W., *et al.* (2004a). Dose-dependent transitions in mechanisms of toxicity: case studies. *Toxicol. Appl. Pharmacol.* **201,** 226–294.

Slikker, W., Jr, Andersen, M. E., Bogdanffy, M. S., Bus, J. S., Cohen, S. D., Conolly, R. B., David, R. M., Doerrer, N. G., Dorman, D. C., Gaylor, D. W., *et al.* (2004b). Dose-dependent transitions in mechanisms of toxicity. *Toxicol. Appl. Pharmacol.* **201,** 203–225.

Sonich-Mullin, C., Fielder, R., Wiltse, J., Baetcke, K., Dempsey, J., Fenner-Crisp, P., Grant, D., Hartley, M., Knaap, A., Kroese, D., *et al.* (2001). IPCS conceptual framework for evaluating a mode of action for chemical carcinogenesis. *Regul. Toxicol. Pharmacol.* **34,** 146–152.

Tan, Y. M., Butterworth, B. E., Gargas, M. L., and Conolly, R. B. (2003). Biologically motivated computational modeling of chloroform cytolethality and regenerative cellular proliferation. *Toxicol. Sci.* **75,** 192–200.

Thompson, C. M., Sonawane, B., Barton, H. A., DeWoskin, R. S., Lipscomb, J. C., Schlosser, P., Chiu, W. A., and Krishnan, K. (2008). Approaches for applications of physiologically based pharmacokinetic models in risk assessment. *J. Toxicol. Environ. Health B Crit. Rev.* **11,** 519–547.

Thrall, K. D., Vucelick, M. E., Gies, R. A., Zangar, R. C., Weitz, K. K., Poet, T. S., Springer, D. L., Grant, D. M., and Benson, J. M. (2000). Comparative metabolism of carbon tetrachloride in rats, mice, and hamsters using gas uptake and PBPK modeling. *J. Toxicol. Environ. Health-Part A* **60,** 531–548.

Trune, D. R., Kempton, J. B., and Gross, N. D. (2006). Mineralocorticoid receptor mediates glucocorticoid treatment effects in the autoimmune mouse ear. *Hear. Res.* **212,** 22–32.

Tsuzuki, T., Egashira, A., Igarashi, H., Iwakuma, T., Nakatsuru, Y., Tominaga, Y., Kawate, H., Nakao, K., Nakamura, K., Ide, F., *et al.* (2001). Spontaneous tumorigenesis in mice defective in the MTH1 gene encoding 8-oxo-dGTPase. *Proc. Natl. Acad. Sci. U.S.A.* **98,** 11456–11461.

U.S. Environmental Protection Agency (USEPA). (2001). *Integrated Risk Information System for Chloroform.* EPA/635/R-01/001. USEPA, Washington, DC. Available at: http://www.epa.gov/NCEA/iris/toxreviews/0025-tr.pdf.

U.S. Environmental Protection Agency (USEPA). (2005). Guidelines for carcinogen risk assessment. EPA/630/P-03/001B. Washington, DC. Available at: http://www.epa.gov/iris/backgr-d.htm.

U.S. Environmental Protection Agency (USEPA). (2008). *Integrated Risk Information System for Carbon Tetrachloride (Publicly Available Draft).* U.S. Environmental Protection Agency, Washington, DC. Available at: http://www.epa.gov/iris/recent_2008.html.

Weibel, E. R., Staubli, W., Gnagi, H. R., and Hess, F. A. (1969). Correlated morphometric and biochemical studies on the liver cell. I. Morphometric model, stereologic methods, and normal morphometric data for rat liver. *J. Cell. Biol.* **42,** 68–91.

Wolf, D. C., and Butterworth, B. E. (1997). Risk assessment of inhaled chloroform based on its mode of action. *Toxicol. Pathol.* **25,** 49–52.

Yamamoto, S., Kasai, T., Matsumoto, M., Nishizawa, T., Arito, H., Nagano, K., and Matsushima, T. (2002). Carcinogenicity and chronic toxicity in rats and mice exposed to chloroform by inhalation. *J. Occup. Health* **44,** 283–293.